Journal of the Franklin Institute 361 (2024) 107198

Contents lists available at ScienceDirect

Journal of the Franklin Institute

journal homepage: www.elsevier.com/locate/fi

Probability hypothesis density filter for parameter estimation of multiple hazardous sources☆

Abdullahi Daniyan [a,*], Cunjia Liu [b], Wen-Hua Chen [b]

[a] Electrical and Electronic Engineering Department, Federal University of Technology, 920211, Minna, Nigeria
[b] Aeronautical and Automotive Engineering Department, Loughborough University, LE11 3TU, United Kingdom

ARTICLE INFO

Keywords:
Source term estimation
Multi-source tracking
Gaussian plume
Plume dispersion
Bayesian estimation
Random finite sets
RFS
Probability hypothesis density
PHD
Sequential Monte Carlo
Particle filtering
Biochemical hazards
Sensor networks
Contaminant source localization
Environmental monitoring

ABSTRACT

This study introduces an advanced methodology for estimating the source term of multiple, variable-number biochemical hazard releases, where the exact count of sources is not predetermined. Focusing on environments monitored via a network of sensors, we tackle this challenge through a multi-source Bayesian filtering paradigm, employing the theory of random finite sets (RFS). Our novel approach leverages a modified particle filter-based probability hypothesis density (PHD) filter within the RFS framework, enabling simultaneous estimation of critical source characteristics (such as location, emission rate, and effective release height) and the quantification of source numbers. This method not only accurately estimates pertinent source parameters but is also adept at identifying the emergence of new sources and the cessation of existing ones within the monitored area. The efficacy of our approach is validated through extensive simulations, which mimic a range of scenarios with varying and unknown source counts, highlighting the proposed method's robustness and precision.

1. Introduction

In source term estimation (STE) for an atmospheric release, the aim is to estimate parameters of interest such as location, release rate/strength, duration, number of sources and other useful parameters that can describe the characteristics of a chemical, biological, and radiological (CBR) release. In the event of a CBR incident, either accidental or deliberate, having a good knowledge of the source parameters could be helpful for early detection and rapid response to the release of the CBR agent. This could in-turn reduce dramatically the extent of human exposure and also minimize the cost of the subsequent associated clean up [1]. It could be possible to deploy an array of CBR concentration sensors within a field of interest to detect contaminant releases. However, mere detection by such sensors may not be sufficient, due to the fact that the detection of a contaminant plume by the sensors only indicates a release has occurred. Having just detection information will not avail us of the characteristics of the source and therefore STE methods are required.

Common STE methods use an array of CBR concentration sensors to provide concentration measurements fused with other information such as meteorological data to estimate the unknown parameters of the source(s). Other STE methods involve the use of mobile robots as concentration sensors, see for example [2]. However, estimation using an array of CBR concentration

☆ This work was supported by the Engineering and Physical Sciences Research Council (EPSRC), United Kingdom Grant number EP/K014307/1.
* Corresponding author.
E-mail addresses: a.daniyan@futminna.edu.ng (A. Daniyan), c.liu5@lboro.ac.uk (C. Liu), w.chen@lboro.ac.uk (W.-H. Chen).

https://doi.org/10.1016/j.jfranklin.2024.107198
Received 30 January 2023; Received in revised form 27 May 2024; Accepted 20 August 2024
Available online 30 August 2024

sensors are usually performed using two main approaches, i.e., probabilistic methods based on Bayesian inference and second, optimization techniques [3]. Both of these approaches aim to find the most likely match between predicted and measured data. These methods mainly achieve this by running inferred source parameters in what is called a forward atmospheric dispersion model to generate predicted concentration data. Using a likelihood function, the predicted concentration data are compared with sensor array measurement to find the most likely fit [3]. Specifically, on the one hand, the optimization-based approaches (see e.g. [4–7]) attempt to find a single optimal solution to the maximum likelihood problem by taking inputs without uncertainty. On the other hand, in Bayesian approaches (see e.g. [8–12]), inputs and models used can be specified using probability density functions while taking into account uncertainties in the input data and the chosen model. With probabilistic inputs, the final output of the algorithm will be in the form of a probability density function, hence, producing an estimate of the source term with associated confidence levels [3]. This attribute makes the Bayesian approaches to STE more suitable for realistic scenarios. Furthermore, the Bayesian framework within the STE context provides a rigorous mathematical foundation for making inferences about the source parameters and thus, provides a rigorous basis for quantifying the uncertainties associated with the estimated source parameters.

The Bayesian inference approach has been applied to solve the STE problem for both the single source release case and the multi-source release case. For the single source case, solutions have been proposed based on different assumptions. For example, the authors in [13,14] proposed a solution for estimating the release rate given that the source location is known; in [15–17] the authors aimed to estimate the source location given that the release rate is known while the authors in [8,9,18,19] proposed a solution for when both the source location and release rate are unknown. Regarding Bayesian STE methods for multiple sources, researches have been focused on estimating different source parameters for multiple sources as well as the number of sources. Most notably are the works of the authors in [20–23] where they proposed solutions to the STE problem for multiple sources based on the Markov chain Monte Carlo (MCMC) principle. However, MCMC methods in general are computationally expensive as they require a large number of particles to perform estimation. Moreover, with MCMC methods, no guarantees exist about it yielding good point estimates [24]. Furthermore, optimization based methods such as genetic algorithm (GA) [25] and least squares (LS) [26] methods have also been used to perform STE for multiple point sources.

Although these methods (i.e. MCMC-based methods, GA and LS) have been applied to the STE problem for multiple point sources, regarding the number of sources estimation, it is interesting to note that only the case where the number of sources are constant but unknown *a priori* has been mainly considered. The case where the number of sources is unknown *a priori* and varies require further attention.

It is desirable and important to know when additional new sources appear within an area of interest during monitoring. Such information could be useful in resource allocation, planning and management. However, in all the previous studies on STE for multiple sources cited here, the focus was on STE for either fixed and known multiple number of sources or fixed and unknown number of sources *a priori*. The case for when the number of sources vary with time still require attention. The problem of determining the number of sources present is a difficult one. More so, the problem becomes even more challenging when the number of sources vary with time.

The relationship between multiple hazardous release sources and the array of CBR sensors within the area of interest can be modelled as a random finite sets (RFS) problem. Under such model, the RFS approach proposed by Mahler, [27] can provide a Bayesian framework for the recursive update of multi-source state posterior density. Under the RFS approach, the source states and the measurements at each time step are modelled as finite set-valued random variables. A framework is available for dealing with as well as characterizing the relative uncertainties in an RFS formulation by using the probabilistic tools of finite sets statistics (FISST) [28]. RFS methods such as the probability hypothesis density (PHD) filter has the potential to solve the problem of source term estimation for multiple sources (STE-MS) especially for the case of varying number of sources. This is inspired by the fact that RFS methods have been used in other fields (e.g. target tracking) to tackle similar problems. The RFS formulation can handle source states and cardinality (i.e. number of sources) estimation especially for appearing and disappearing in a recursive Bayesian filter problem. A common RFS method is the PHD filter. The PHD filter is a recursion that propagates the posterior intensity of an RFS in time [27,29]. The integral of a PHD is the expected number of objects in a measurable region, and the peaks of the PHD function provide the estimates of the object states [29]. The PHD filter has successfully applied in various fields to achieve state and object number estimation in both simulation and real world applications. These application areas include: radar tracking [30], acoustic source tracking [31], sonar image tracking [32], simultaneous localization and mapping (SLAM) [33], distributed multi-target tracking [34], tracking with millimetre-wave images [35], tracking with target amplitude feature information [36] and sinusoidal components tracking in audio [37].

In this work, the CBR context considered is for the specific case of biochemical releases. Previous researches into the use of Bayesian framework to solve the STE-MS problem have focused mainly on particle filtering and MCMC methods [3]. These methods primarily considered the case where the number of sources were unknown but fixed and unchanging. However, in this paper, we propose a new paradigm for STE of multiple hazardous releases for the challenging case of varying number of sources using the random finite set approach. We refer to this technique as the STE-MS-probability hypothesis density (STE-MS-PHD) filter. In our approach, we model the STE-MS problem as a multi-source Bayes filtering problem and use a random finite sets approach to solve the problem. Specifically, we use the particle filter implementation of the random finite sets-based probability hypothesis density filter to jointly perform multiple source state and number of sources estimation.

This paper presents three main contributions:

1 We redefine the issue of estimating source terms for multiple hazardous sources (STE-MS) with an unknown and variable number of sources as a multi-source Bayes filtering challenge. By employing the Bayesian framework, we not only establish a solid mathematical groundwork for deducing source parameters, but also a method to measure uncertainties. This structure further enables us to apply Bayesian estimation techniques.

2 Our solution for the multi-source Bayes STE-MS challenge employs the random finite sets method within the finite set statistics framework. By using this method, we can represent both the states of multiple sources and the multiple observations from sensors as random sets with a finite number of elements. This is particularly beneficial as it can adjust to a changing number of elements, making it apt for estimating variables with differing cardinalities.
3 For a combined estimation of multiple source states and the fluctuating number of contaminant sources, we adopt the particle version of the random finite sets-based probability hypothesis density filter. We chose the particle implementation of this filter since there is a non-linear relationship between the source parameters we are examining and the observed data on concentration.

The remainder of the paper is organized as follows. In Section 2, we describe the problem considered in this paper along with providing a contextual background. Section 3 presents a brief background information on Bayesian multi-source inference and the likelihood functioned used in the paper. We introduce the proposed random finite sets-based probability hypothesis density filter for STE-MS along with related background derivations in Section 4. Section 5 contain simulation results highlighting the improvements offered by our proposed technique followed by concluding remarks in Section 6.

2. Problem formulation

2.1. Context

Consider a rectangular area of interest $\Omega \in \mathbb{R}^2$ in which one or more hazardous releases are expected to be present. The rectangular field is equipped with R static sensors whose locations are known and fixed. These sensors are able to detect and measure contamination concentrations. These sensors provide the necessary inputs to a multiple-source estimator to estimate the number of sources and parameters of interest about the source (e.g. location, release rate, etc.). Each sensor $r^{(i)}$ (where $i = 1, \dots, R$) output a concentration reading $y^{(i)} \in \mathbb{R}^+$ that can be related to the concentration of hazardous material in the air. This concentration measurement from all sensors can be used to predict the parameters of the source, i.e. the source term. The source term can include several parameters that depend on the type of release and the models used to forecast the dispersion. In this work, the source term of the release is parametrized by:

- cartesian coordinates θ of the source.
- effective release height H of the source.
- release rate/strength Q of the source, and
- the number N of sources present.

Hence, the parameter vector of the source term at time k can be defined as:

$$\boldsymbol{\Theta}_k = [\boldsymbol{X}_k, N_k], \quad \boldsymbol{X}_k = \{\boldsymbol{x}_k^j\}_{j=1}^{N_k}, \quad \boldsymbol{x}_k^j = [\boldsymbol{\theta}_k^j, Q_k^j, H_k^j]^T. \tag{1}$$

The ith sensor outputs observations $y_{1:K}^{(i)} = \{y_1^{(i)}, \dots, y_K^{(i)}\}$ from the hazardous sensor at discrete time steps $k = 1, \dots, K$; where $1:K$ denotes from time $k = 1$ upto and including time $k = K$. It is assumed that each source, when present has a release rate, Q^j which is normally distributed with mean μ_Q^j and standard deviation σ_Q^j, i.e. $\mathcal{N}(\mu_Q^j, \sigma_Q^j)$.. At each time step k, the multi-source estimator updates its estimates of the source parameters $\boldsymbol{x}_k$.

2.2. Dispersion modelling

In this work, we assume that for each source (when present) disperses a contaminant plume according to the time-varying Gaussian plume dispersion model. Therefore the concentration at time k at a given sensor location with coordinates $(\tilde{x}^{(i)}, \tilde{y}^{(i)}, \tilde{z}^{(i)})$ due to a source located at $(\check{x}_j, \check{y}_j, \check{z}_j)$ having release rate $Q_j(k)$ is given below

$$C(\bar{x}, \bar{y}, \bar{z}, k)_j = \frac{Q_j(k)}{2\pi u(k)\sigma_{\bar{y}}(k)\sigma_{\bar{z}}(k)} \exp\left(-\frac{\bar{y}^2}{2\sigma_{\bar{y}}(k)^2}\right)\left[\exp\left(-\frac{(\bar{z}-H_j)^2}{2\sigma_{\bar{z}}(k)^2}\right) + \exp\left(-\frac{(\bar{z}+H_j)^2}{2\sigma_{\bar{z}}(k)^2}\right)\right], \tag{2}$$

where $\sigma_{\bar{y}}(k) = 465.11628 \cdot \bar{x} \cdot \tan(\vartheta(k))$, $\vartheta(k) = 0.017453293(c(k) - d(k)\ln(\bar{x}))$, $\sigma_{\bar{z}} = a(k)\bar{x}^{b(k)}$, $\bar{x} = \tilde{x}^{(i)} - \check{x}_j$, $\bar{y} = \tilde{y}^{(i)} - \check{y}_j$ and $\bar{z} = \tilde{z}^{(i)} - \check{z}_j$ are the downwind, crosswind and vertical distances; $\sigma_{\bar{y}}$ denotes the atmospheric turbulence coefficient, $\sigma_{\bar{z}}$ represents the standard deviations that describe the crosswind and vertical mixing of the contaminant; u is the mean wind speed at the height H_j of the release and a and b are variables that depend on $\bar{x}$ and c and d are parameters that depend on six vertical atmospheric stability categories (which are very unstable, moderately unstable, slightly unstable, neutral, moderately stable and very stable) [38]. The standard deviations $\sigma_{\bar{y}}$ and $\sigma_{\bar{z}}$ depend on the atmospheric stability category. In unstable conditions the standard deviations rapidly increase downwind and stable conditions have standard deviations that stay small downwind.

3. Multi-source estimation

Building upon the previously defined state vectors of interest in (1), let $\boldsymbol{x} = [\theta, Q, H]^T$ represent such a vector, where θ, Q, and H have been defined earlier. Consider a set of state vectors $\boldsymbol{x}_1, \ldots, \boldsymbol{x}_N$, with each $\boldsymbol{x}_j$ belonging to the state space $\mathcal{X} \subseteq \mathbb{R}^d$. Here, $\mathcal{X}$ denotes the collection of all possible state vectors that can occur, and d is the dimension of the state space. Let $y^{(i)}$ denote the observation at the ith sensor. The value $y^{(i)}$ of the ith sensor can be a real number or a vector depending on the application. Given sensor observations $\{y^{(i)}\}_{i=1}^{R}$, we consider the problem of jointly estimating the number of sources and their states (e.g. location and release rate).

Firstly, we formulate a suitable representation of the multi-source state and cast the estimation problem in a Bayesian framework in Section 3.1. The observation model and the likelihood function considered in this paper is then described in Section 3.2, setting the scene for the main results in Section 4.

3.1. Bayesian multi-source inference

Generally, in the Bayesian estimation, the state and measurement are treated as realizations of random variables. Given that the multi-source state $\boldsymbol{X}$ in our problem is a finite set whose elements are random variables, the concept of a random finite set is required to cast this multi-source estimation problem in the Bayesian framework. The space of finite subsets of $\mathcal{X}$ does not inherit the usual Euclidean notion of integration and density and therefore, standard tools used for random vectors cannot be appropriate for RFSs [39]. However, Mahler's technique known as finite set statistics provides powerful yet practical mathematical tools for dealing with RFSs [27,28], based on a notion of integration and density that is consistent with point process theory [40]. FISST has attracted substantial interest from academia as well as the commercial sector with the developments of the probability hypothesis density (PHD) and cardinalized PHD filters [27,28,40–43].

Using the FISST notion of integration and density, the posterior probability density $p(\cdot \mid y^{(i)})$ of the multi-source state can be computed from the prior p using Bayes rule

$$p(\boldsymbol{X} \mid y^{(i)}) = \frac{g(\boldsymbol{y} \mid \boldsymbol{X}) p(\boldsymbol{X})}{\int g(\boldsymbol{y} \mid \boldsymbol{X}) p(\boldsymbol{X}) \delta \boldsymbol{X}} \tag{3}$$

where $p(\boldsymbol{X})$ denotes the prior probability density function (pdf) of the multi-source state $\boldsymbol{X}$ that encapsulates the current state of knowledge of the parameters before receiving the concentration measurements; $g(\boldsymbol{y} \mid \boldsymbol{X})$ denotes the likelihood function and is the probability density of the observation $\boldsymbol{y}$ given the multi-source state $\boldsymbol{X}$; the denominator on the right-hand-side of (3) denotes the evidence, which is also referred to as the marginal or prior predictive likelihood; $p(\boldsymbol{X} \mid y^{(i)})$ denotes the posterior probability density function of the multi-source state of interest $\boldsymbol{X}$, that corresponds to the update of the prior $p(\boldsymbol{X})$ incorporating the knowledge gained about $\boldsymbol{X}$ after receiving the concentration observations $\boldsymbol{y}$.

3.2. Multi-source likelihood function

Consider the problem formulation described in Section 2. Let $y_k^{(i)}$ be the concentration datum measured by sensor $r^{(i)}$ at time k. Given the contaminant dispersion model of (2), the predicted concentration measurement, $\hat{y}_k^{(i)}$, by the sensor $r^{(i)}$ is given as:

$$\hat{y}_k^{(i)} = \sum_{j=1}^{N} C(\bar{x}, \bar{y}, \bar{z})_{j,k} + e_k \tag{4}$$

where N is the number of sources, e_k denotes the error associated with the predicted concentration measurement and is assumed to be Gaussian distributed with zero mean and covariance of Σ_o, i.e. $\mathcal{N}(0, \Sigma_o)$.

The likelihood function for a sensor in a multi-source scenario quantifies how likely it is to observe the data given a set of model parameters. For a single sensor $r^{(i)}$ at time k, the likelihood of observing the concentration datum $y_k^{(i)}$ given the model parameters and the state of the sources can be formulated based on the Gaussian distribution assumption for the measurement noise.

Given that the Gaussian plume model of (2) is Gaussian and the predicted concentration measurement of (4) for each source and assuming the measurement noise is normally distributed, the likelihood function for sensor $r^{(i)}$ at time k is:

$$g(y_k^{(i)} | \boldsymbol{x}_k) = \frac{1}{\sqrt{2\pi\sigma_\eta^2}} \exp\left(-\frac{(\hat{y}_k^{(i)} - y_k^{(i)})^2}{2\sigma_\eta^2} \right) \tag{5}$$

where $g(y_k^{(i)} | \boldsymbol{x}_k)$ is the likelihood of the measurement $y_k^{(i)}$, $\boldsymbol{x}_k$ represents the source parameters, $\hat{y}_k^{(i)}$ is the estimated concentration at sensor $r^{(i)}$ at time k, reflecting the aggregate influence of all sources plus the measurement noise, and σ_η is the standard deviation of the measurement noise.

This likelihood function captures the probability of observing the concentration measurements at each sensor, taking into account the source parameters. However, the diversity in the sensors' data regarding granularity, precision, and volume means that assimilating observations into a singular set may hinder convergence during filtering. Consequently, to ensure more robust estimations, observations from each sensor are processed independently, with their filtering outcomes fused subsequently under the framework of FISST. This approach enhances the estimation of source parameters within a Bayesian framework based on the data collected.

3.3. Sensing mechanism

Various chemical detectors are capable of measuring the concentration of biochemical substances in the atmosphere. However, due to the intrinsic limits of biochemical sensors, a sensor will not output reading if the concentration level is less than the sensor's threshold. To account for this, a distance-dependent sensor threshold $\tau^{(i)}$ is used, which takes into account the proximity of all sources to the sensor and is inversely proportional to a weighted average of the distances from the expected source locations. This threshold is applied to the measurement model defined in Eq. (4) as follows:

$$\hat{y}_k^{(i)} = \begin{cases} \hat{y}_k^{(i)}, & \text{if} \quad \hat{y}_k^{(i)} > \tau^{(i)} \\ 0, & \text{if} \quad \hat{y}_k^{(i)} \leq \tau^{(i)}. \end{cases} \tag{6}$$

A sensor $r^{(i)}$ is only triggered when the predicted measurement $\hat{y}_k^{(i)}$ is greater than the threshold $\tau^{(i)}$, which is calculated as:

$$\tau^{(i)} = \frac{\tau_0}{1 + \alpha d^{(i)}} \tag{7}$$

$$d^{(i)} = \sum_{j=1}^{N_k} u_j^{(i)} \left\| \mathbf{r}^{(i)} - \mathbf{x}_k^j \right\| \tag{8}$$

Here, τ_0 is a base threshold, α is a proportionality constant that determines how quickly the threshold decreases with distance, and $d^{(i)}$ is the weighted average distance between the sensor $r^{(i)}$ and all N_k sources present at time k. The weights $u_j^{(i)}$ are proportional to the predicted contribution of each source j to the total concentration $\hat{y}_k^{(i)}$ at sensor $r^{(i)}$, and are calculated as:

$$u_j^{(i)} = \frac{C(\bar{x}, \bar{y}, \bar{z})_{j,k}}{\sum_{l=1}^{N_k} C(\bar{x}, \bar{y}, \bar{z})_{l,k}}$$

Here, $C(\bar{x}, \bar{y}, \bar{z})_{j,k}$ is the contribution of the jth source to the predicted concentration $\hat{y}_k^{(i)}$ at sensor $r^{(i)}$ and time k, as given by the Gaussian plume model in Eq. (2).

4. Multiple source filtering using the probability hypothesis density filter

This section considers the multi-source filtering problem for multiple hazardous release. In particular, the problem of the on-line estimation of the state of multiple sources and the number of the sources from measured concentration data based on the random finite set formulation is treated. The random finite set approach represents the multi-source state as a finite set of single-source states, and the multi-source estimation problem is formulated as a dynamic multi-source state estimation problem.

In what follows, the idea of random finite set is presented in Section 4.1 and the probability hypothesis density filter introduced in Section 4.2. We describe the multi-source state space model and multi-source Bayes recursion in Sections 4.3 and 4.4 respectively. Lastly, the probability hypothesis density filter introduced in Section 4.5.

4.1. Random finite set

A random finite set (RFS) can be defined as a finite-set-valued random variable. The RFS Λ, of $\mathcal{Z}$, is a random variable taking values in $\mathcal{F}(\mathcal{Z})$, the collection of all finite subsets of $\mathcal{Z}$. The finite set statistic (FISST) notion of integration/density is used to characterize RFSs [28]. In an RFS, the number of points is random; the points themselves are random and unordered as opposed to a random vector. The FISST density of an RFS Λ is a non-negative function ξ on $\mathcal{F}(\mathcal{Z})$ such that for any region $S \subseteq \mathcal{F}(\mathcal{Z})$,

$$\Pr(\Lambda \subseteq S) = \int_S \xi(\Lambda) \delta\Lambda \tag{9}$$

where the above integral is a set integral which is defined as [27]:

$$\int \xi(\Lambda) \delta\Lambda = \sum_{i=0}^{\infty} \frac{1}{i!} \int_{S^i} \xi(\{z_1, \ldots, z_i\}) d(z_1, \ldots, z_i). \tag{10}$$

This means that the set integral of the FISST density over a region S, yields the probability that Λ is contained in the region S [39,40].

4.2. The PHD

Given an RFS Λ, its first order moment is termed the probability hypothesis density (PHD). The PHD is also known as the intensity function [27]. The PHD, $D_\Lambda(\boldsymbol{x})$ of an RFS Λ is given by [27,28,44]:

$$D_\Lambda(\boldsymbol{x}) = \mathbf{E}\left\{\delta_\Lambda(\boldsymbol{x})\right\} = \int \delta_{\boldsymbol{X}}(\boldsymbol{x}) P_\Lambda(d\boldsymbol{X}) \tag{11}$$

where $\mathbf{E}\{\cdot\}$ is the statistical expectation operator and $\delta_\Lambda(\mathbf{x}) = \sum_{\mathbf{y} \in \Lambda} \delta_{\mathbf{y}(\mathbf{x})}$ is the random density representation of Λ. P_Λ is the probability measure of the RFS.

4.3. Multi-source state and multi-source observation space model

In systems where the object of interest is a single object, the uncertainty in such a system is characterized by modelling the states and measurements by random vectors [39]. However, in cases where objects of interest are more than one (multi-objects), the random vector modelling cannot hold. Therefore, uncertainty in such cases are characterized by modelling multi-object states and multi-object measurements as RFSs. In our formulation, the objects of interest are the multiple sources releasing biochemical contaminant into the atmosphere. So, let the multi-source state set be $\boldsymbol{X}_k$ on the state space. Given the non-homogeneous nature of the sensor data in our problem, we do not bundle observations from all sensors to form an observation set. Instead, we consider each sensor individually. Consequently, let the multi-source measurements be $y^{(i)}_{1:K}$ on the observation space E_o, where 'from $k = 1$ to $k = K$' denotes the time period from the initial time $k = 1$ up to and including the final time $k = K$.

In our problem, the multi-source state at time k is modelled by the RFS

$$\boldsymbol{X}_k = S_k(\boldsymbol{X}_{k-1}) \cup B_k \tag{12}$$

where $S_k(\boldsymbol{X}_{k-1})$ denotes the RFS of sources that have persisted/survived at time k, B_k is the RFS of new sources that appear spontaneously at time k.

In a similar manner, we could model the multi-source observation from the ith sensor by the RFS

$$\boldsymbol{Y}^{(i)}_k = y^{(i)}_k(\boldsymbol{X}_k) \cup C_k \tag{13}$$

where $y^{(i)}_k(\boldsymbol{X}_k)$ denotes the measurements generated by $\boldsymbol{X}_k$ at the ith sensor, and C_k denotes the RFS of false alarms. Generally, in RFS applications such as target tracking, false alarms are included in the measurement observation model to account for detections not due to targets of interest. In our problem, given that measurements are in the form of concentration/intensity data, the concept of false alarms/clutter naturally does not apply. However, our inclusion of false alarm in our measurement model is to capture the possibility of a faulty sensor reporting measurement where there is not a source.

4.4. Multi-source Bayes recursion

Our multi-source filtering problem can be cast as a Bayes filtering one on the space of finite sets $\mathcal{F}(\mathcal{Z})$. Generally, Bayesian multi-object estimation is carried out using two stages, prediction and update. In our problem, the multi-source prediction from time $k-1$ to time k is given by the Chapman–Kolmogorov equation

$$p_{k|k-1}(\boldsymbol{X}_k|\boldsymbol{Y}^{(i)}_{1:k-1}) = \int f_{k|k-1}(\boldsymbol{X}_k|\boldsymbol{X}) p_{k-1}(\boldsymbol{X}|\boldsymbol{Y}^{(i)}_{1:k-1}) \delta\boldsymbol{X}, \tag{14}$$

where $f_{k|k-1}(\boldsymbol{X}_k|\boldsymbol{X})$ encapsulates all aspects of the multi-source parameters such as the time-varying number of sources, individual source dynamics, and new source births. The update equation at the ith sensor is given by

$$p(\boldsymbol{X}_k \mid \boldsymbol{Y}^{(i)}_{1:k}) = \frac{g_k(\boldsymbol{Y}^{(i)}_k \mid \boldsymbol{X}_k) p_{k|k-1}(\boldsymbol{X}_k|\boldsymbol{Y}^{(i)}_{1:k-1})}{\int g_k(\boldsymbol{Y}^{(i)}_k \mid \boldsymbol{X}_k) p_{k|k-1}(\boldsymbol{X}_k|\boldsymbol{Y}^{(i)}_{1:k-1}) \delta\boldsymbol{X}}. \tag{15}$$

Both (14) and (15) form collectively form the multi-source Bayes recursion. However, (14)–(15) is generally intractable, and therefore approximations are required in order to derive practical algorithms [28]. One of such approximations is the RFS-based probability hypothesis density filter which is presented next.

4.5. The PHD filter

The PHD filter is an inexpensive and computationally efficient approximation of the multi-object Bayes filter which was derived by the authors in [27] using FISST. The PHD filter is a recursion of the PHD, $D^{(i)}_{k|k}$ that is associated with the multi-source posterior density $p(\boldsymbol{X}_k \mid \boldsymbol{Y}^{(i)}_k)$ such that

$$p(\boldsymbol{X}_k \mid \boldsymbol{Y}^{(i)}_k) \propto g(\boldsymbol{Y}^{(i)}_k \mid \boldsymbol{X}_k) p(\boldsymbol{X}_k|\boldsymbol{Y}^{(i)}_{k-1}) \tag{16}$$

where $p(\boldsymbol{X}_k|\boldsymbol{Y}^{(i)}_{k-1})$ and $g(\boldsymbol{Y}^{(i)}_k \mid \boldsymbol{X}_k)$ denotes the multi-source prior and likelihood density respectively. Since we are using sensor-wise observations, we will be processing the PHD of each sensor separately and subsequently fusing their filtering outcomes.

The prediction equation of the PHD of the ith sensor, $D^{(i)}_{k|k}$ in our problem is:

$$D^{(i)}_{k|k-1}(\boldsymbol{x}_k|\boldsymbol{Y}^{(i)}_{k-1}) = \gamma_k(\boldsymbol{x}_k) + \int \phi_{k|k-1}(\boldsymbol{x}_k, \boldsymbol{x}_{k-1}) D_{k-1|k-1}(\boldsymbol{x}_{k-1}|\boldsymbol{Y}^{(i)}_{k-1}) d\boldsymbol{x}_{k-1}. \tag{17}$$

The term $\phi_{k|k-1}(\boldsymbol{x}_k, \boldsymbol{x}_{k-1})$ is given as

$$\phi_{k|k-1}(\boldsymbol{x}_k, \boldsymbol{x}_{k-1}) = p_S(\boldsymbol{x}_{k-1}) f_{k|k-1}(\boldsymbol{x}_k, \boldsymbol{x}_{k-1}), \tag{18}$$

where $p_S(\cdot)$ is the probability of the source survival, $f_{k|k-1}(\boldsymbol{x}_k, \boldsymbol{x}_{k-1})$ is the single source dynamics model, $\gamma_k(\cdot)$ is the PHD for spontaneous birth.

The classical PHD filter update equation for a "standard" measurement model where it is assumed that no object generates more than one measurement per time step, and no measurement is generated by more than one object is given as:

$$D^{(i)}_{k|k}(\boldsymbol{x}_k|\boldsymbol{Y}^{(i)}_k) = \left[1 - p_D(\boldsymbol{x}_k)\right] D^{(i)}_{k|k-1}(\boldsymbol{x}_k|\boldsymbol{Y}^{(i)}_{k-1}) + \left[\sum_{\boldsymbol{Y}^{(i)}_k} \frac{p_D(\boldsymbol{x}_k) g(y^{(i)}|\boldsymbol{x}_k)}{\kappa_k(y^{(i)}) + \langle D^{(i)}_{k|k-1}, p_D(\boldsymbol{x}_k) g(y^{(i)}|\boldsymbol{x}_k)\rangle}\right] D^{(i)}_{k|k-1}(\boldsymbol{x}_k|\boldsymbol{Y}^{(i)}_{k-1}), \tag{19}$$

where $p_D(\boldsymbol{x}_k)$ denotes the probability of source detection. The term $g(y^{(i)}|\boldsymbol{x}_k)$ is the measurement likelihood function for the single source; $\kappa_k(y^{(i)})$ is the false alarm intensity and $\langle \cdot, \cdot \rangle$ denotes inner product operator.

However, given that measurement model in our problem is not "standard" but superpositional in nature, we apply the superpositional PHD update equation below [45,46]:

$$D^{(i)}_{k|k}(\boldsymbol{x}_k|\boldsymbol{Y}^{(i)}_k) = \psi(\boldsymbol{Y}^{(i)}_k|\boldsymbol{x}_k) D^{(i)}_{k|k-1}(\boldsymbol{x}_k|\boldsymbol{Y}^{(i)}_{k-1}) \tag{20}$$

$$\psi(\boldsymbol{Y}^{(i)}_k|\boldsymbol{x}_k) = \frac{\mathcal{N}(\boldsymbol{Y}^{(i)}_k - \hat{y^{(i)}}_k - \mu_k, \Sigma_o + \Sigma_k)}{\mathcal{N}(\boldsymbol{Y}^{(i)}_k - \mu_k, \Sigma_o + \Sigma_k)} \tag{21}$$

$$\mu_k = \int \hat{y^{(i)}}_k \delta \boldsymbol{x}_k \tag{22}$$

where $\hat{y^{(i)}}_k$ denotes the projection of the source state from the state space onto the measurement space. This refers back to (2).

4.6. Particle PHD filter for multi-source parameter estimation

The PHD filter can be implemented in two fashions, either using the Gaussian mixture (GM-PHD) method or using the sequential Monte Carlo (SMC) approach (particle PHD). Under a linear and Gaussian model, the PHD filter admits a closed form solution in the form of the GM-PHD filter. The SMC-PHD filter or particle PHD filter is an effective estimation technique in non-linear and non-Gaussian scenarios because filtering and estimation is carried out using random set of weighted particles.

In our problem, given that the relationship between the source parameters of interest and the observed concentration data as seen in (2) is non-linear, we adopt the particle implementation of the PHD filter to solve our problem. The prediction and update stages of the particle PHD filter we implemented are presented next. This is followed by a description of how the number of sources are estimated and how the source states are extracted post filtering.

It is worth noting here that the standard PHD filter is known to have a high variance in its cardinality estimation especially when the number of objects is high. However, the Cardinalized Probability Hypothesis Density (CPHD) filter [47] was developed to address this challenge. The SMC PHD filter for the multi-source parameter estimation proposed here can be easily extended to the CPHD filter version. this can be achieved by jointly the cardinality distribution in addition to the number of sources and their states. But for the focus of this paper is on the PHD filter.

4.6.1. The prediction operator

It is implicit from our measurement and likelihood model in (4) and (5) that we assume that our likelihood model and measurement does not affect the prediction step of the standard PHD filter. Therefore, the predicted PHD, $D^{(i)}_{k|k-1}$ for our problem is:

$$D^{(i)}_{k|k-1}(\boldsymbol{x}_k|\boldsymbol{Y}^{(i)}_{k-1}) = \sum_{l=1}^{\mathcal{L}_k} w^l_{k|k-1} \delta_{\boldsymbol{x}^l_{k|k-1}}(\boldsymbol{x}_k), \tag{23}$$

where $\mathcal{L}_k = L_{k-1} + J_k$ and L_{k-1} and J_k are two sets of particles drawn from two proposal densities to represent existing and newly appeared sources respectively as:

$$\boldsymbol{x}^l_{k|k-1} \approx \begin{cases} q_k(\cdot|\boldsymbol{x}^l_{k-1}, \boldsymbol{Y}^{(i)}_k), & l = 1, \ldots, L_{k-1} \\ p_k(\cdot|\boldsymbol{Y}^{(i)}_k), & l = L_{k-1}+1, \ldots, \mathcal{L}_k. \end{cases} \tag{24}$$

These particles have corresponding weights:

$$w^l_{k|k-1} = \begin{cases} \frac{\phi_{k|k-1}(\boldsymbol{x}^l_k, \boldsymbol{x}^l_{k-1})}{q_k(\boldsymbol{x}_{k|k-1}|\boldsymbol{x}^l_{k-1}, \boldsymbol{Y}^{(i)}_k)} w^l_{k-1}, & l = 1, \ldots, L_{k-1} \\ \frac{\gamma_k(\boldsymbol{x}^l_k)}{J_k p_k(\boldsymbol{x}_{k|k-1}|\boldsymbol{Y}^{(i)}_k)}, & l = L_{k-1}+1, \ldots, \mathcal{L}_k \end{cases} \tag{25}$$

where $p_k(\cdot|\cdot)$ and $q_k(\cdot|\cdot)$ denote the proposal distributions for newly appeared sources and existing sources respectively; $p_S(\cdot)$ is the probability of source survival, $\gamma_k(\cdot)$ is the PHD of the spontaneous birth, and J_k is the number of particles for newly appeared sources.

4.6.2. The update operator

For each ith sensor, with observed measurement $y_k^{(i)}$ let

$$\mu_k = \sum w_{k|k-1}^{l} \hat{y^{(i)}}_{k,l},$$
$$\Sigma_k = \sum w_{k|k-1}^{l} (\hat{y^{(i)}}_{k,l})^T (\hat{y^{(i)}}_{k,l}), \tag{26}$$

then, for $l = 1, \ldots, \mathcal{L}_k$, update the weights using:

$$w_k^l = \left[\frac{\mathcal{N}(\boldsymbol{Y}_k^{(i)} - \hat{y^{(i)}}_{k,l} - \mu_k, \Sigma_o + \Sigma_k)}{\mathcal{N}(\boldsymbol{Y}_k^{(i)} - \mu_k, \Sigma_o + \Sigma_k)} \right] w_{k|k-1}^{l}, \tag{27}$$

where $\hat{y^{(i)}}_{k,l}$ denotes the projection of the lth particle from the state space onto the measurement space, μ_k denotes how well do the other particles describe the current observed measurement if no source is present at the lth particle position and Σ_k is the measure of the associated uncertainty. Thus, the updated PHD, $D_{k|k}^{(i)}$ is then given as:

$$D_{k|k}^{(i)}(\boldsymbol{x}_k | \boldsymbol{Y}_k^{(i)}) = \sum_{l=1}^{\mathcal{L}_k} w_k^l \delta_{\boldsymbol{x}_k^l}(\boldsymbol{x}_k) \tag{28}$$

4.6.3. PHD fusion

After applying the PHD filter to each sensor's data, the results were fused using Generalized Covariance Intersection (GCI) thus:

$$D_{k|k}^{fused}(\boldsymbol{x}_k | \boldsymbol{Y}_k^{(i)}) = \frac{\prod_{i=1}^{R} [D_{k|k}^{(i)}(\boldsymbol{x}_k | \boldsymbol{Y}_k^{(i)})]^{\omega_i}}{\int \prod_{i=1}^{R} [D_{k|k}^{(i)}(\boldsymbol{x}_k | \boldsymbol{Y}_k^{(i)})(\xi)]^{\omega_i} d\xi} \tag{29}$$

Here, $D_{k|k}^{fused}(\boldsymbol{x}_k | \boldsymbol{Y}_k^{(i)})$ is the fused intensity function, $D_{k|k}^{(i)}(\boldsymbol{x}_k | \boldsymbol{Y}_k^{(i)})$ is the intensity function from the i-th sensor, R is the number of sensors, and ω_i are the non-negative weights that sum to one and reflect the relative confidence in each sensor's data. The weights ω_i were chosen based on the inverse of the sensor's measurement variance. The denominator ensures that the fused intensity function is properly normalized.

4.6.4. Number of sources

The expected number of sources $N_{k|k}$ is computed as:

$$N_{k|k} = \text{round}\left(\sum_{f=1}^{\mathcal{F}_k} w_k^f \right) \tag{30}$$

where round$(\cdot)$ denotes round to the nearest integer and $\mathcal{F}_k$ denote the total of all fused sensor particles at time k.

4.6.5. Resampling

In order to avoid degeneracy where a few set of particles dominate other particles with their weights, $\mathcal{F}_k = \rho N_{k|k}$ particles are resampled using particle resampling techniques such as the improved systematic resampling [48]. The number of resampled particles $\mathcal{F}_k$ is determined based on the effective sample size and is typically set to a fraction of the total number of particles to maintain diversity and accuracy.

After resampling, the particles $\mathcal{F}_k$ are distributed among the sensors for the next recursion. The number of particles $\mathcal{L}_{k+1}$ for each sensor is proportional to the confidence in the sensor's measurements and the weights assigned during the fusion process. This relationship is defined as:

$$\mathcal{L}_{k+1}^{(i)} = \omega_i \cdot \mathcal{F}_k \tag{31}$$

where ω_i is the weight assigned to the ith sensor based on its measurement variance. The weights ω_i are computed as follows:

$$\omega_i = \frac{\frac{1}{\sigma_i^2}}{\sum_{j=1}^{R} \frac{1}{\sigma_j^2}} \tag{32}$$

where σ_i^2 is the measurement variance of the ith sensor and R is the total number of sensors. This ensures that the resampling process maintains the balance between particle diversity and the accuracy of the state estimation.

4.6.6. Source state extraction

Following the resampling step, the estimated source states can be extracted. This can be done by first estimating the number of sources as the expected or maximum *a posteriori* cardinality estimate, and then estimating the individual states by selecting the corresponding number of the means or modes from the state or source term densities. The number of sources can already be obtained according to (30). As for the mean selection, this can be achieved using clustering techniques such as K-means clustering to cluster the resampled particles given the number of sources.

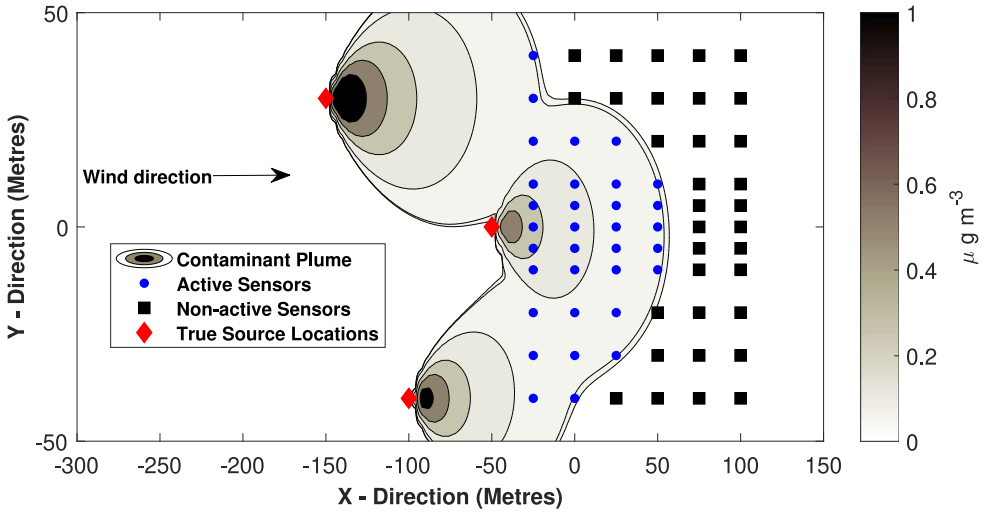

Fig. 1. Contaminant release from three fixed sources. True source locations are indicated by red-coloured diamond shape. Sensors that have been triggered due to contaminant plume from the sources are shown as blue-coloured dots while non-triggered sensors are shown as black-coloured squares.

Table 1
Example I: Source profiles.

S/N	Along-wind x, (m)	Cross-wind y, (m)	Rate, Q (g/s)
1	−150	30	1
2	−50	0	0.3
3	−100	−40	0.6

5. Simulation

In this section, we demonstrate the performance of our proposed technique for the source term estimation of multiple sources using the PHD filter. For this purpose, we consider two simulation examples where simulated concentration data will be generated in order to estimate source parameters of interest. In the first example, we used our proposed method to perform STE for fixed but unknown number of sources *a priori*. For this example, we compared the performance of our method with the Bayesian-MCMC (B-MCMC) method proposed in [1,9,49] using various metrics. In the second example, we considered the STE-MS problem for when the number of sources are unknown and vary. In this instance, we illustrate and assess the effectiveness of the STE-MS-PHD filter alongside its CPHD filter equivalent, employing a variety of performance indicators. The efficacy of the STE-MS-PHD filter was benchmarked against that of the STE-MS-CPHD filter.

In both of the simulation examples, each source when present is assumed to follow the dynamic model below:

$$\boldsymbol{x}_k = \boldsymbol{x}_{k-1} + \boldsymbol{v}_k \tag{33}$$

where $\boldsymbol{v}_k$ is an independent and identically distributed Gaussian noise with zero mean and covariance Σ.

5.1. Example I

Consider a field of interest of dimensions $[-200\ \text{m}, 150\ \text{m}] \times [-50\ \text{m}, 50\ \text{m}]$ equipped fixed position concentration sensors as shown Fig. 1. There are a total of 66 sensors whose locations are fixed and known. These sensors are able to pick up and measure contaminant concentrations and serve as measurement sources to both the B-MCMC STE-MS estimator and the STE-MS-PHD filter. For this case, a total of three hazardous sources are present and are emitting continuous plumes at different rates within the field of interest. The number, release rate and position of these sources are assumed to be unknown to both the STE-MS methods used. The source profile of the three sources are given in Table 1. It is assumed that all sensors have a height of $z = 1$ m above the ground. Each source is assumed to have an effective source height, $H = 2$ m and the wind speed in this example is assumed to be $u = 6$ m/s. Therefore, in this simulation example, the relevant source parameters of interest are the source locations ($\boldsymbol{\theta} = \{x, y\}$) and the release rate ($Q$). The measurement noise level used in this example was 10% of the true measurement data.

The birth space for the STE-MS-PHD method was set as the dimension of the field of interest for the source coordinates and [0 to 10] for the release rate. The B-MCMC method was initialized by generating random samples from $[-50\ \text{m}, 50\ \text{m}]$, $[-200\ \text{m}, 150\ \text{m}]$ and [0 to 10] for the x, y and Q components respectively. The minimum and maximum expected number of sources for the B-MCMC method was set as 1 and 8 respectively.

Table 2
Estimate of source parameters.

Source	Parameter	Truth	RMSE	
			STE-MS-PHD	B-MCMC
1	x (m)	−150	4.533	6.710
	y (m)	30	4.362	5.393
	Q (g s^{-1})	1	0.144	0.163
2	x (m)	−50	3.154	4.085
	y (m)	0	1.741	2.108
	Q (g s^{-1})	0.3	0.307	0.472
3	x (m)	−100	4.565	5.712
	y (m)	−40	4.229	5.570
	Q (g s^{-1})	0.6	0.275	0.398

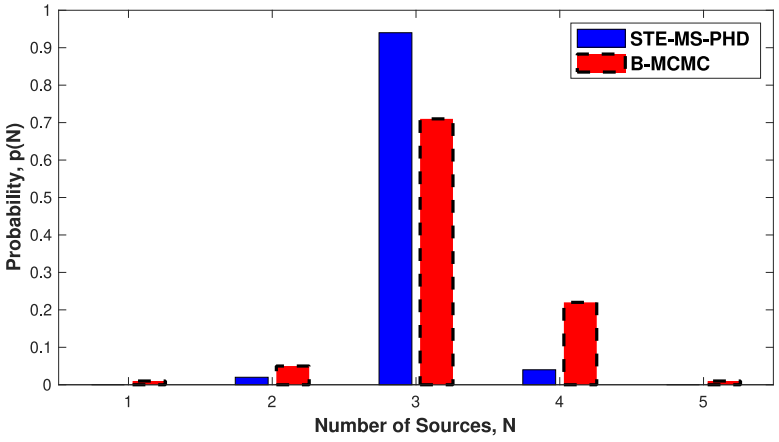

Fig. 2. Posterior distribution for the estimated number of sources.

To evaluate performance of both the B-MCMC STE-MS estimator and the STE-MS-PHD filter in this example, we use the root mean squared error (RMSE), probability of correctly estimating the number of sources, execution time (ET) and the optimal subpattern assignment distance [50] between the estimated and true multi-source states. The results presented are averaged over 100 Monte Carlo (MC) simulations. The RMSE is computed individually for each source parameter as

$$\text{RMSE}_n = \sqrt{\frac{1}{N}\sum_{i=1}^{N}(\boldsymbol{a}_i^n - \hat{\boldsymbol{a}}_i^n)^2} \tag{34}$$

where n in $\boldsymbol{a}_i^n$ denotes the nth source, $\boldsymbol{a} = \{x, y, Q\}$, i denotes the index of the elements in $\boldsymbol{a}$ and N is the number of sources; $\{\boldsymbol{a}_i^n\}_{i=1}^{N}$ denotes the ground truth of the nth source and $\left\{\hat{\boldsymbol{a}}_i^n\right\}_{i=1}^{N}$ denotes the nth source estimates.

Table 2 shows the RMSE computation results obtained from applying both the B-MCMC STE-MS estimator and the STE-MS-PHD filter. It can be observed from the Table that both methods are able to estimate the source parameters of interest, namely, the x and y locations of each source along with their release rates, Q. However, it is observed from the table that the estimation error for the release rate is particularly high for both methods, especially for the sources with low release rates, i.e., for sources 2 and 3. The STE-MS-PHD filter consistently shows lower RMSE values for the spatial parameters (x and y) compared to the B-MCMC method, highlighting its effectiveness in these estimations.

With regards to the estimate of the number of sources by both methods, we computed the probability of each method correctly estimating the true number of sources in 100 MC trials. Fig. 2 shows the result obtained from the evaluation. We see that the STE-MS-PHD method is able to correctly estimate the number of sources 94% of the time while the B-MCMC method is able to correctly estimate the true number of sources 70% of the time.

We also considered the ET required to execute a single run of each of the methods when different number of particles are used. From Fig. 3, we see that the B-MCMC method requires more ET to execute when compared to the STE-MS-PHD method. This could be due to the number of burn-in samples required by the B-MCMC method during execution.

Fig. 4 presents a comparison of source cardinality estimation over time between the two methods against the true number of sources. The solid line represents the actual number of active sources, the dashed blue line represents the cardinality estimated by the STE-MS-PHD filter, and the dashed red line represents the cardinality estimated by the B-MCMC method. It is observed that both methods experience some deviation from the true number of sources, with the STE-MS-PHD filter showing closer alignment

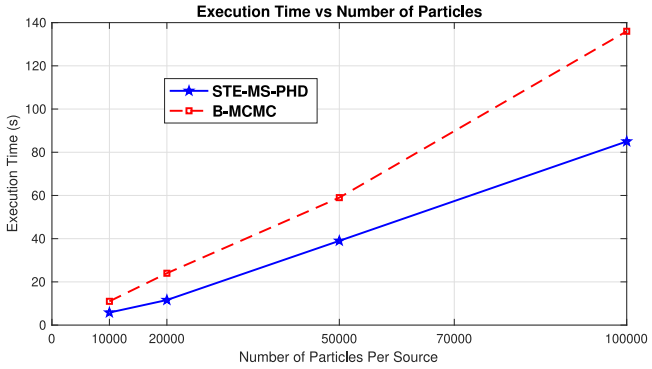

Fig. 3. Estimator performance evaluation in terms of ET versus varying number of particles time averaged over 100 MC trials.

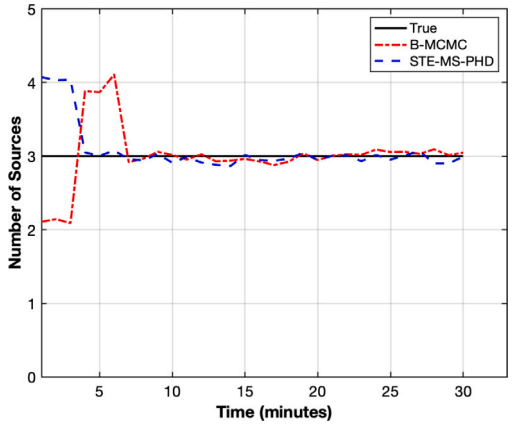

Fig. 4. Cardinality estimation comparison time averaged over 100 MC trials.

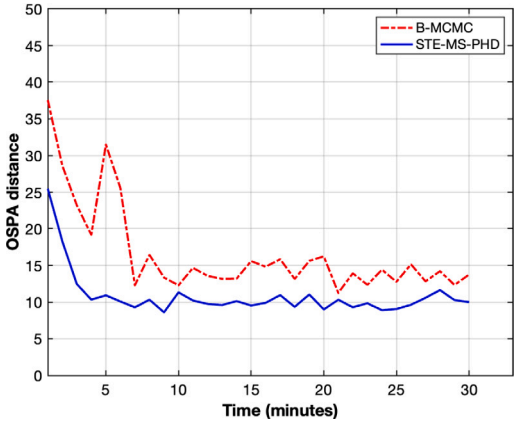

Fig. 5. OSPA distance evaluation time averaged over 100 MC trials.

overall. Particularly at the beginning, both methods show some fluctuation but the STE-MS-PHD method appears to stabilize more quickly and closely track the true cardinality throughout the remainder of the time.

Fig. 5 illustrates the OSPA distances for the STE-MS-PHD and B-MCMC methods over time, measuring combined errors in cardinality and position estimates. The solid blue line indicates the OSPA distance for the STE-MS-PHD method, while the dashed red line corresponds to the B-MCMC method. Initially, the B-MCMC method exhibits a high OSPA distances, suggesting larger estimation errors. In contrast, the STE-MS-PHD method, despite starting with high errors, demonstrates a significant reduction in OSPA distance as time progresses, consistently outperforming the B-MCMC method in terms of accuracy and reliability.

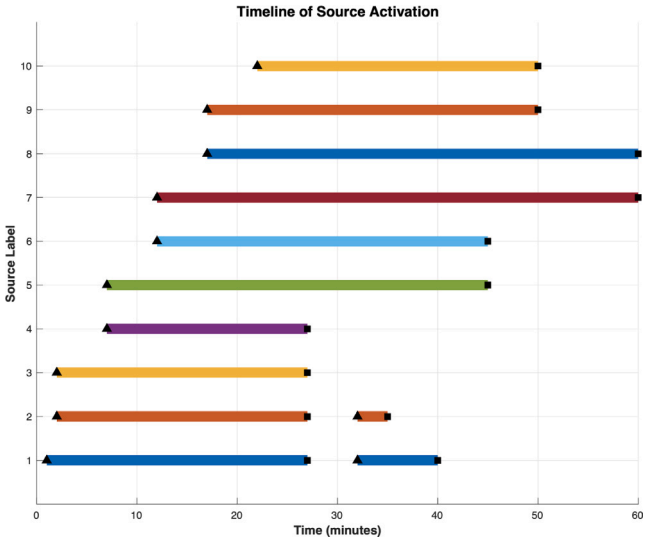

Fig. 6. Active periods of all sources over time. Each line represents the activity duration of a source, marked by unique colours for easy identification. The triangle markers indicate the start times, while the square markers denote the end times of the active periods for each source.

Table 3
Source profiles.

Source	X-Location, (m)	Y-Location, (m)	Mean rate, Q (g/s)	Effective height, H
1	−1761	2032	182	0.98
2	−1216	2358	999	0.60
3	972	1686	1011	0.83
4	2231	933	909	0.9
5	−342	857	1437	1.32
6	1103	412	1528	1.48
7	161	−248	1211	0.57
8	−1509	−536	130	0.76
9	−2451	2215	890	1.13
10	861	−2376	800	1.11

5.2. Example II

5.2.1. Set up

A field of interest with dimensions [5 km × 5 km] equipped with 49 fixed position concentration sensors whose locations are known. These sensors are able to pick up and measure contaminant concentrations and serve as measurement sources to both the STE-MS-PHD filter and its CPHD counterpart.

We generate a synthetic dataset according to the time-varying Gaussian plume model of (2). As for the wind vertical stability, we considered the case of *very unstable* stability of the Pasquill–Gifford–Turner [38,51,52] vertical stability class models. In the simulation model, sources can appear and die out within the field of interest at any time. During the simulation period, a total of 10 contaminant sources were present at various times. However, this information is assumed to be unknown *a priori*.

The source profile of the 10 sources are given in Table 3. It is assumed that all the sensors have a height $z = 0$, i.e. at ground level. Each source is assumed to have an effective source height, H and the wind speed u in this example is assumed to be in the range [2 m/s to 4 m/s]. Therefore, the relevant source parameters of interest are the source locations (θ), the release rate (Q) and the effective height (H). The simulation duration was 60 min.

Fig. 7 shows the synthetic contaminant data generated from our simulation model where the source profiles of Table 3 and Fig. 6 were utilized. The Figure illustrates emissions from ten sources at time $k = 25$. From the Figure, sensors that have detected emissions are marked with red asterisks (*), while those that have not are represented by black dots. Notice from the Figure that the plumes from the sources spread out and become wider, and as a result, more sensors are triggered and more measurements are available due to the emissions from the sources. Also, observe the overlapping plumes from different sources.

5.2.2. Multi-source miss distance

In order to evaluate the estimation error of our proposed approach, we use the optimal subpattern assignment (OSPA) distance [50] between the estimated and true multi-source states as the estimation error. This section briefly describes a concept for

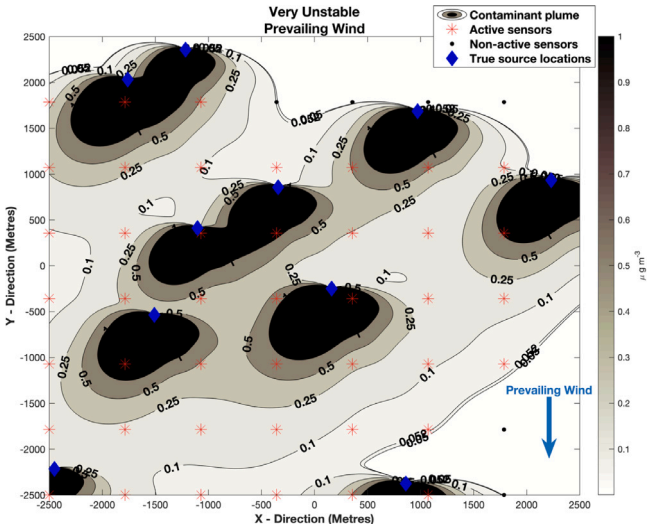

Fig. 7. Source emissions at time $k = 25$. True source locations are indicated by blue-coloured diamond shape. Sensors that have been triggered due to contaminant plume from the sources are shown as red-coloured asterisk while non-triggered sensors are shown as black-coloured dots.

computing error between two sets based on the OSPA formulation. This way, we can jointly capture the differences in individual elements and cardinality between two finite sets in a way that is intuitively meaningful and mathematically consistent.

The OSPA distance between two arbitrary finite sets $\mathbf{A} = \{\mathbf{a}_1, \ldots, \mathbf{a}_m\}$ and $\mathbf{B} = \{\mathbf{b}_1, \ldots, \mathbf{b}_n\}$ is presented as follows:

$$\bar{d}_p^{(c)}(\mathbf{A}, \mathbf{B}) = \begin{cases} 0 & \text{if} \quad m = n = 0 \\ \Psi(\mathbf{A}, \mathbf{B}) & \text{if} \quad m \leq n \\ d^{(c)}(\mathbf{A}, \mathbf{B}) & \text{if} \quad m > n \end{cases} \tag{35}$$

where

$$\Psi(\mathbf{A}, \mathbf{B}) \triangleq \left(\frac{1}{n} \left(\min_{\pi \in \prod_n} \sum_{i=1}^{m} d^{(c)}(a_i, b_{\pi(i)})^p + c^p(n - m) \right) \right)^{\frac{1}{p}} \tag{36}$$

$d^{(c)}(\mathbf{a}, \mathbf{b}) := \min\{c, \| \mathbf{a} - \mathbf{b} \|\}$ is the distance between single target vectors $\mathbf{a}$ and $\mathbf{b}$; $\prod_n$ is the set of permutations with length m on the set $\{1, \ldots, n\}$; $c > 0$ is the cut-off parameter and $p \geq 1$ is a unit-less real number. We choose parameters $c = 100$ and $p = 1$. The parameter p determines the sensitivity to outliers and the cut-off parameter c determines the relative weighting of the penalties assigned to localization and cardinality errors. For more details on the OSPA metric, the reader is referred to [50].

5.2.3. Results

Table 4 provides a comparison between the true source parameters and the estimates obtained from both filters for all ten sources. The parameters estimated are the x and y coordinates (in meters), which represent the location of the sources, the effective release height H (in meters), and the release rate Q (in grams per second, g s^{-1}). For each source, the true values are compared to the estimates from the STE-MS-PHD filter and its CPHD filter counterpart. The STE-MS-PHD filter provides a close approximation of the true source parameters. However, there are discrepancies between the estimated and true values, which is expected due to limitations in the modelling and data. The STE-MS-CPHD filter also provides estimates of the source parameters. The performance of the STE-MS-CPHD filter is quite similar to that of the PHD filter, with minor variations in the estimated values. Additionally, from the table, we see that the estimation accuracy for the STE-MS-CPHD filter is slightly higher when compared to that of the STE-MS-PHD filter. Since both filters work in a similar manner to obtain the state estimate, the higher accuracy seen with the STE-MS-CPHD filter could be due to the better cardinality estimate offered by the CPHD filter.

We further evaluated our method's performance using the OSPA metric and the OSPA sub-index. On the one hand, the OSPA metric jointly quantifies the estimation errors in terms of position and cardinality while the OSPA sub-index on the other hand separately quantify the errors in cardinality and position, providing two distinct measures. Fig. 8 shows the OSPA result obtained when we applied our proposed method, the STE-MS-PHD and its CPHD filter counterpart. As depicted in the Figure, the application of our proposed filters yielded comparatively low OSPA values. The Figure illustrates periodic spikes for both methods, with the STE-MS-PHD filter exhibiting spikes of higher magnitude relative to the CPHD filter. These spikes align with instances when the number of sources changes. The CPHD filter's spikes are less pronounced, reflecting its capability to jointly estimate the cardinality distribution and position of the sources. Notably, between time points 27 and 30, where a sharp decline in the number of sources occurs, the STE-MS-PHD filter exhibits a delayed adjustment in comparison to the CPHD filter.

Table 4
Estimate of source parameters.

Source	Parameter	Truth	Estimates	
			STE-MS-PHD	STE-MS-CPHD
1	x (m)	−1716	−1690	−1740
	y (m)	2032	2100	1999
	H (m)	0.98	1.01	0.92
	Q (g s^{-1})	1579	1430	1510
2	x (m)	−1216	−1241	−1226
	y (m)	2358	2337	2321
	H (m)	0.60	0.72	0.69
	Q (g s^{-1})	674	731	707
3	x (m)	972	1003	994
	y (m)	1686	1632	1675
	H (m)	0.83	0.91	0.78
	Q (g s^{-1})	1372	1297	1347
4	x (m)	2231	2186	2253
	y (m)	933	923	912
	H (m)	0.9	1.01	0.83
	Q (g s^{-1})	1393	1270	1313
5	x (m)	−342	−307	−324
	y (m)	857	832	861
	H (m)	1.32	1.10	1.01
	Q (g s^{-1})	1061	994	1001
6	x (m)	1103	1092	1117
	y (m)	412	401	422
	H (m)	1.48	1.22	1.27
	Q (g s^{-1})	927	877	903
7	x (m)	161	153	159
	y (m)	−248	−221	−232
	H (m)	0.57	0.81	0.63
	Q (g s^{-1})	1970	1913	1991
8	x (m)	−1509	−1483	−1531
	y (m)	−536	−519	−527
	H (m)	0.76	0.87	0.81
	Q (g s^{-1})	1475	1417	1448
9	x (m)	−2451	−2390	−2411
	y (m)	2215	2195	2225
	H (m)	1.13	1.10	1.10
	Q (g s^{-1})	587	472	503
10	x (m)	861	900	893
	y (m)	−2376	−2311	−2348
	H (m)	1.11	1.01	0.99
	Q (g s^{-1})	1590	1447	1498

Figs. 9 and 10 present the OSPA sub-index metrics for cardinality and localization errors, respectively. Fig. 9 demonstrates the temporal evolution of cardinality errors, with the dashed red line representing the STE-MS-PHD method's cardinality error and the solid blue line representing the true cardinality. Fig. 10 depicts the localization errors over time, with the same colour scheme. Both figures underscore the individual estimation errors, with the STE-MS-PHD method's error trends indicating its performance in estimating the number of sources and their positions over the duration of the observation period.

Figs. 11 and 12 depict the cardinality estimate performance of the two filtering methods over time. In both figures, the blue solid line represents the actual number of active sources (ground truth), the dashed red line indicates the estimated number of sources by the filters, and the shaded grey area shows the plus or minus one standard deviation of the source number estimate obtained from the filters.

In Fig. 11, the STE-MS-PHD filter closely follows the ground truth with some deviations, particularly noticeable where the source cardinality changes. The filter's uncertainty is depicted by the STD region. The STE-MS-PHD filter shows a delay in adapting to the changes in source numbers around the 30-minute mark where there was an abrupt cardinality decrease.

Fig. 12, also displays the tracking of active source cardinality, with a similar pattern of the STE-MS-PHD filter closely following the actual number of sources and the CPHD filter's uncertainty is depicted by the STD region. As expected, the CPHD filter's STD region suggests that its cardinality estimates have a lesser degree of uncertainty in its estimate of number of sources.

For both filters, the cardinality estimate tends to be more uncertain during periods of change in the number of sources. Both filters generally maintain a close approximation to the true cardinality but displays some lag in response to changes, which is particularly evident in Fig. 11. The CPHD filter, while generally encompassing the true cardinality within its STD bounds, illustrates lesser variability and uncertainty in its estimation process.

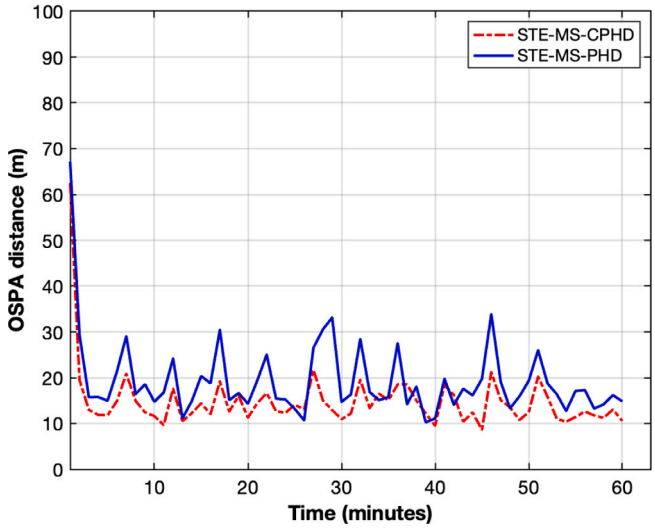

Fig. 8. Estimator performance evaluation in terms of OSPA distance time averaged over 100 MC trials.

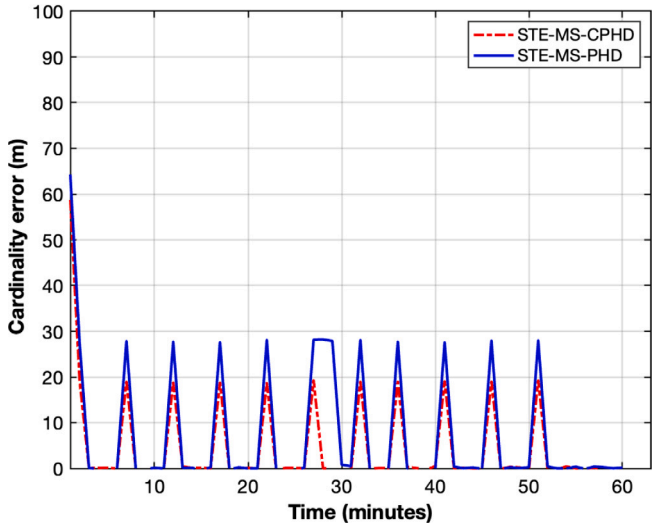

Fig. 9. OSPA distance sub index: Cardinality component time averaged over 100 MC trials.

6. Conclusions

We have developed and demonstrated a novel approach for multi-source term estimation that effectively copes with time-varying and initially unknown and varying number of sources, utilizing noisy sensor data within a random finite sets framework. Our method, termed the STE-MS-PHD filter, incorporates the PHD filter implemented through a particle filter, addresses the non-linearity between observed data and source parameters. Simulation studies have confirmed the accuracy of our method in estimating both the number of sources and their parameters, aligning closely with the ground truth, and its capability to detect the advent and disappearance of sources dynamically. Future work will aim at applying this method to experimental data, further affirming its practical applicability and refining its real-world performance.

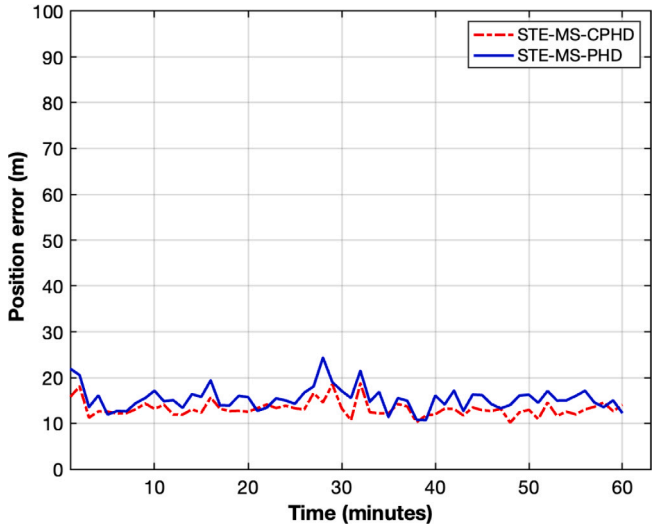

Fig. 10. OSPA distance sub index: Localization component time averaged over 100 MC trials.

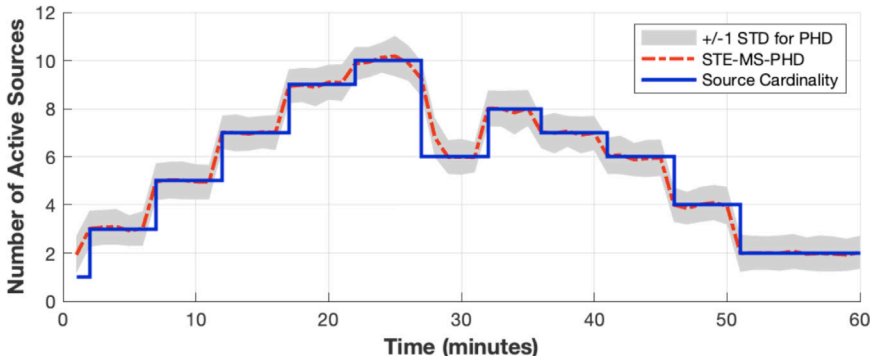

Fig. 11. True number of sources, STE-MS-PHD filter estimates and ±1 standard deviation of the filter estimate time averaged over 100 MC trials.

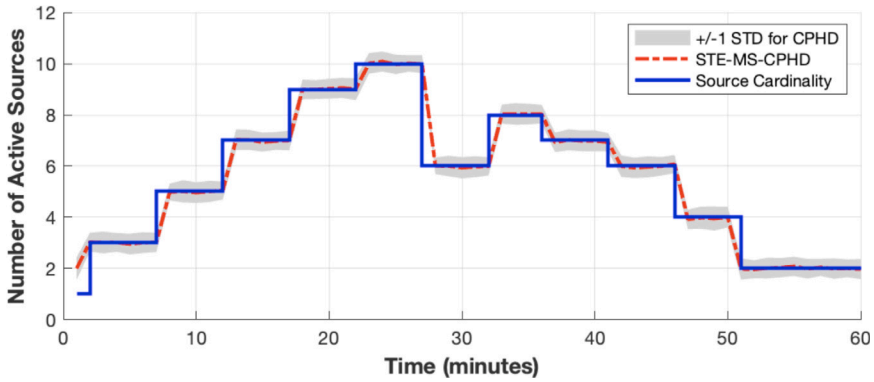

Fig. 12. True number of sources, STE-MS-CPHD filter estimates and ±1 standard deviation of the filter estimate time averaged over 100 MC trials.

CRediT authorship contribution statement

Abdullahi Daniyan: Conceptualization, Data curation, Formal analysis, Investigation, Methodology, Software, Validation, Visualization, Writing – original draft, Writing – review & editing. **Cunjia Liu:** Conceptualization, Funding acquisition, Project administration, Resources, Supervision, Validation, Writing – review & editing. **Wen-Hua Chen:** Conceptualization, Funding acquisition, Project administration, Resources, Supervision, Writing – review & editing.

Declaration of competing interest

The authors declare that they have no known competing financial interests or personal relationships that could have appeared to influence the work reported in this paper.

References

[1] E. Yee, Bayesian Inversion of Concentration Data for an Unknown Number of Contaminant Sources, Tech. Rep., Defence Research and Development Suffield (Alberta), 2007.
[2] M. Hutchinson, C. Liu, W. Chen, Information-based search for an atmospheric release using a mobile robot: Algorithm and experiments, IEEE Trans. Control Syst. Technol. (2018) 1–15, http://dx.doi.org/10.1109/TCST.2018.2860548.
[3] M. Hutchinson, H. Oh, W.-H. Chen, A review of source term estimation methods for atmospheric dispersion events using static or mobile sensors, Inf. Fusion 36 (2017) 130–148.
[4] S.E. Haupt, G.S. Young, C.T. Allen, A genetic algorithm method to assimilate sensor data for a toxic contaminant release, J. Comput. Phys. 2 (6) (2007) 85–93.
[5] K.J. Long, S. Haupt, G.S. Young, L.M. Rodriguez, M. McNeal III, Source term estimation using genetic algorithm and SCIPUFF, in: 7th Conference on Artificial Intelligence and Its Applications to the Environmental Sciences, 2009.
[6] X. Zheng, Z. Chen, Back-calculation of the strength and location of hazardous materials releases using the pattern search method, J. Hazard. Mater. 183 (1–3) (2010) 474–481.
[7] S.K. Singh, R. Rani, A least-squares inversion technique for identification of a point release: application to fusion field trials 2007, Atmos. Environ. 92 (2014) 104–117.
[8] A. Keats, E. Yee, F.-S. Lien, Bayesian inference for source determination with applications to a complex urban environment, Atmos. Environ. 41 (3) (2007) 465–479.
[9] E. Yee, Bayesian probabilistic approach for inverse source determination from limited and noisy chemical or biological sensor concentration measurements, in: Chemical and Biological Sensing VIII, Vol. 6554, International Society for Optics and Photonics, 2007, 65540W.
[10] B. Ristic, A. Gunatilaka, R. Gailis, Localisation of a source of hazardous substance dispersion using binary measurements, Atmos. Environ. 142 (2016) 114–119.
[11] B. Ristic, A. Gunatilaka, Y. Wang, Rao–Blackwell dimension reduction applied to hazardous source parameter estimation, Signal Process. 132 (2017) 177–182.
[12] B. Ristic, A. Gunatilaka, R. Gailis, A. Skvortsov, Bayesian likelihood-free localisation of a biochemical source using multiple dispersion models, Signal Process. 108 (2015) 13–24.
[13] S. Kaharabata, P. Schuepp, R. Desjardins, Source strength determination of a tracer gas using an approximate solution to the advection–diffusion equation for microplots, Atmos. Environ. 34 (15) (2000) 2343–2350.
[14] Y.N. Skiba, On a method of detecting the industrial plants which violate prescribed emission rates, Ecol. Model. 159 (2–3) (2003) 125–132.
[15] J. Matthes, L. Groll, H.B. Keller, Source localization by spatially distributed electronic noses for advection and diffusion, IEEE Trans. Signal Process. 53 (5) (2005) 1711–1719.
[16] A. Khapalov, Localization of unknown sources for parabolic systems on the basis of available observations, Int. J. Syst. Sci. 25 (8) (1994) 1305–1322.
[17] M.E. Alpay, M.H. Shor, Model-based solution techniques for the source localization problem, IEEE Trans. Control Syst. Technol. 8 (6) (2000) 895–904.
[18] J.A. Pudykiewicz, Application of adjoint tracer transport equations for evaluating source parameters, Atmos. Environ. 32 (17) (1998) 3039–3050.
[19] E. Yee, A Bayesian approach for reconstruction of the characteristics of a localized pollutant source from a small number of concentration measurements obtained by spatially distributed "electronic noses", in: Russian-Canadian Workshop on Modeling of Atmospheric Dispersion of Weapon Agents, Karpov Institute of Physical Chemistry, Moscow, Russia, 2006.
[20] D. Wade, I. Senocak, Stochastic reconstruction of multiple source atmospheric contaminant dispersion events, Atmos. Environ. 74 (2013) 45–51.
[21] R. Lane, M. Briers, K. Copsey, Approximate Bayesian computation for source term estimation, Math. Def. (2009).
[22] C. Huang, T. Hsing, N. Cressie, A.R. Ganguly, V.A. Protopopescu, N.S. Rao, Bayesian source detection and parameter estimation of a plume model based on sensor network measurements, Appl. Stoch. Models Bus. Ind. 26 (4) (2010) 331–348.
[23] E. Yee, Inverse dispersion for an unknown number of sources: model selection and uncertainty analysis, ISRN Appl. Math. 2012 (2012).
[24] Z. Khan, T. Balch, F. Dellaert, MCMC-based particle filtering for tracking a variable number of interacting targets, IEEE Trans. Pattern Anal. Mach. Intell. 27 (11) (2005) 1805–1819.
[25] A.J. Annunzio, G.S. Young, S.E. Haupt, A multi-entity field approximation to determine the source location of multiple atmospheric contaminant releases, Atmos. Environ. 62 (2012) 593–604.
[26] S.K. Singh, R. Rani, Assimilation of concentration measurements for retrieving multiple point releases in atmosphere: a least-squares approach to inverse modelling, Atmos. Environ. 119 (2015) 402–414.
[27] R.P.S. Mahler, Multitarget Bayes filtering via first-order multitarget moments, IEEE Trans. Aerosp. Electron. Syst. 39 (4) (2003) 1152–1178, http://dx.doi.org/10.1109/TAES.2003.1261119.
[28] R.P. Mahler, Statistical Multisource-Multitarget Information Fusion, Artech House, Inc., 2007.
[29] A. Daniyan, Y. Gong, S. Lambotharan, P. Feng, J. Chambers, Kalman-gain aided particle PHD filter for multitarget tracking, IEEE Trans. Aerosp. Electron. Syst. 53 (5) (2017) 2251–2265, http://dx.doi.org/10.1109/TAES.2017.2690530.
[30] S. Tian, Y. He, G. Wang, PHD filter of multi-target tracking with passive radar observations, in: 2006 8th International Conference on Signal Processing, Vol. 4, IEEE, 2006.
[31] B. Balakumar, A. Sinha, T. Kirubarajan, J. Reilly, PHD filtering for tracking an unknown number of sources using an array of sensors, in: 2005 IEEE/SP 13th Workshop onStatistical Signal Processing, IEEE, 2005, pp. 43–48.
[32] D.E. Clark, Multiple Target Tracking with the Probability Hypothesis Density Filter (Ph.D. thesis), Heriot-Watt University, 2006.
[33] J. Mullane, B. Vo, M.D. Adams, W.S. Wijesoma, A PHD filtering approach to robotic mapping, in: IEEE Conf. on Control, Automation, Robotics and Vision, 2008.

[34] T. Li, V. Elvira, H. Fan, J.M. Corchado, Local diffusion based distributed SMC-PHD filtering using sensors with limited sensing range, IEEE Sens. J. (2018) 1, http://dx.doi.org/10.1109/JSEN.2018.2882084.
[35] C.D. Haworth, Y. De Saint-Pern, D. Clark, E. Trucco, Y.R. Petillot, Detection and tracking of multiple metallic objects in millimetre-wave images, Int. J. Comput. Vis. 71 (2) (2007) 183–196.
[36] D. Clark, B. Ristic, B.-N. Vo, PHD filtering with target amplitude feature, in: 2008 11th International Conference OnInformation Fusion, IEEE, 2008, pp. 1–7.
[37] D. Clark, A.-T. Cemgil, P. Peeling, S. Godsill, Multi-object tracking of sinusoidal components in audio with the Gaussian mixture probability hypothesis density filter, in: 2007 IEEE Workshop on Applications of Signal Processing to Audio and Acoustics, IEEE, 2007, pp. 339–342.
[38] D.B. Turner, Workbook of Atmospheric Dispersion Estimates: An Introduction to Dispersion Modeling, CRC Press, 1994.
[39] B.-N. Vo, M. Mallick, Y. Bar-Shalom, S. Coraluppi, R. Osborne III, R. Mahler, B.-T. Vo, Multitarget tracking, Wiley Encycl. Electr. Electron. Eng. (2015).
[40] B.-N. Vo, S. Singh, A. Doucet, Sequential Monte Carlo methods for multitarget filtering with random finite sets, IEEE Trans. Aerosp. Electron. Syst. 41 (4) (2005) 1224–1245, http://dx.doi.org/10.1109/TAES.2005.1561884.
[41] B.-N. Vo, W.-K. Ma, The Gaussian mixture probability hypothesis density filter, IEEE Trans. Signal Process. 54 (11) (2006) 4091–4104.
[42] B.T. Vo, B.N. Vo, A. Cantoni, Analytic implementations of the cardinalized probability hypothesis density filter, IEEE Trans. Signal Process. 55 (7) (2007) 3553–3567, http://dx.doi.org/10.1109/TSP.2007.894241.
[43] R. Mahler, PHD filters of higher order in target number, IEEE Trans. Aerosp. Electron. Syst. 43 (4) (2007) 1523–1543, http://dx.doi.org/10.1109/TAES.2007.4441756.
[44] R. Mahler, "Statistics 102" for multisource-multitarget detection and tracking, IEEE J. Sel. Top. Sign. Proces. 7 (3) (2013) 376–389.
[45] S. Nannuru, M. Coates, R. Mahler, Computationally-tractable approximate PHD and CPHD filters for superpositional sensors, IEEE J. Sel. Top. Sign. Proces. 7 (3) (2013) 410–420.
[46] R. Mahler, CPHD filters for superpositional sensors, in: Signal and Data Processing of Small Targets 2009, Vol. 7445, International Society for Optics and Photonics, 2009, 74450E.
[47] B.-T. Vo, B.-N. Vo, A. Cantoni, The cardinalized probability hypothesis density filter for linear Gaussian multi-target models, in: 2006 40th Annual Conference on Information Sciences and Systems, 2006, pp. 681–686, http://dx.doi.org/10.1109/CISS.2006.286554.
[48] A. Daniyan, Y. Gong, S. Lambotharan, An improved resampling approach for particle filters in tracking, in: 2017 22nd International Conference on Digital Signal Processing, DSP, 2017, pp. 1–5, http://dx.doi.org/10.1109/ICDSP.2017.8096095.
[49] E. Yee, Validation of a Bayesian inferential framework for multiple source re-construction using FFT-07 data, in: HARMO13-1-4 June 2010, Paris, France-13 Th Conference on Harmonisation within Atmospheric Dispersion Modeling for Regulatory Purposes, 2010.
[50] D. Schuhmacher, B.-T. Vo, B.-N. Vo, A consistent metric for performance evaluation of multi-object filters, IEEE Trans. Signal Process. 56 (8) (2008) 3447–3457.
[51] F. Pasquill, The estimation of the dispersion of windborne material, Meteorol. Mag. 90 (1961) 33–49.
[52] F.A. Gifford, Use of routine meteorological observations for estimating atmospheric dispersion, Nucl. Saf. 2 (1961) 47–51.